ChemComm

Accepted Manuscript

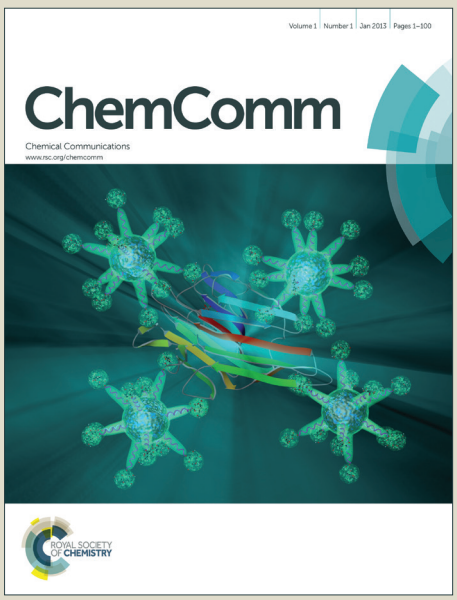

ROYAL SOCIETY OF CHEMISTRY

www.rsc.org/chemcomm

Journal Name

RSCPublishing

COMMUNICATION

Designing Two-Photon Fluorescent Probes Based on Target-Induced Enhancement of Absorption Cross Section

Cite this: DOI: 10.1039/x0xx00000x

Received 00th January 2012,
Accepted 00th January 2012

DOI: 10.1039/x0xx00000x

www.rsc.org/

Lingyu Zeng, ‡[a] Shiyu Chen, ‡[a] Tian Xia, [b] Cheng Zhong [c] and Zhihong Liu*[a]

We reported a new strategy to design two-photon (2P) fluorescent probes for simultaneous elevation of 2P absorption cross section (δ) and quantum yield (ϕ). The target-induced hydrogen bond-chelated ring enhances molecular planarity, leading to enhancement of δ; meanwhile, the photo-induced electron transfer (PET) "on-off" process modulates ϕ.

Two-photon (2P) fluorescent probes are powerful tools for imaging in living systems.[1] Compared with one-photon (1P) microscopy, 2P microscopy features larger penetration depth, lower autofluorescence, less photodamage to biological samples and reduced photobleaching of dyes. Nonetheless, the progress in this field is restricted by the development of 2P fluorescent probes with high efficiencies.[2] To guarantee sensitive response in sensing and imaging, 2P fluorescent probes need to exhibit significant change of 2P active cross section, which is the product of fluorescence quantum yield (ϕ) and 2P absorption cross section (δ), when responding to targets.[3] Some electronic processes like intramolecular charge transfer (ICT), photo-induced electron transfer (PET) and resonance energy transfer (RET) have been well established as design strategies for 2P fluorescent probes, through which the ϕ is modulated.[4] It should be stressed that 2P probes exceptionally depend on another parameter δ, which is decisive for the absorption and photoluminescence of 2P molecules.[5] However, to the best of our knowledge, so far the reported 2P fluorescent probes all focused on promotion of ϕ upon target reaction, while the enhancement of δ has not been utilized.

Reports on both theoretical[6] and experimental[7] studies illustrated that molecular planarity is a vital positive factor to elevate δ of two-photon absorption (2PA) molecules. Inspired by this, we herein report a new strategy to design 2P fluorescent probes with enlarged δ after the probe-target reaction, which is realized by employing fluorophore with excited state intramolecular proton transfer (ESIPT) property. Molecules with ESIPT property can undergo an intrinsic enol-keto phototautomerization, providing applicability in proton transfer lasers, organic light-emitting diodes and ratiometric fluorescent probes.[8] It is particularly worth noting that in ESIPT molecules the intramolecular hydrogen bond can form five- or six-membered rings, which will help to lock the molecule in a coplanar structure.[8b,9] There are a few ESIPT molecules reported with non-linear optical property and some showed 2PA characteristic.[10] These facts gave us a hint that it would be possible to increase δ during target sensing if an ESIPT "off-on" switch can be integrated into a 2P probe. To this end, we prepared compounds **1a**-**1c** (Scheme 1) to find a proper moiety for designing 2P fluorophores with ESIPT property. Further, we constructed the 2P fluorescent probe **2a** (and its reference molecule **2b**) to achieve the probe-target reaction-induced simultaneous enhancement of both ϕ and δ.

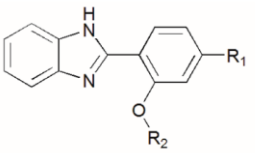

compound	R_1	R_2
1a	H	H
1b	OMe	H
1c	NEt_2	H
2a	NEt_2	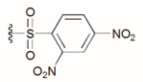
2b	NEt_2	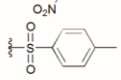

Scheme 1 Structures of compound **1a**~**1c** and **2a**~**2b**

We started from the development of an appropriate 2P fluorophore with ESIPT property, adopting 2-(2'-hydroxyphenyl)benzimidazole (HBI, **1a**), a known ESIPT molecule[10d] as the fluorescent moiety. **1a** has rather short absorption wavelength (main absorption peak at 320 nm in DMSO, Table S1), which is in principle not an ideal scaffold for 2P fluorophores. To

improve its 2PA property, we synthesized **1b** and **1c** with substitution at R_1 position by electron-donating groups to construct D-π-A electronic configuration, a typical structure to increase the molecular dipole in 2PA molecule design. (D: electron donor; A: electron acceptor). Compared to **1a**, the absorption peak of **1b** shows slight shift to 336 nm while **1c** displays obvious red-shift to 360 (Table S1). The longest absorption wavelength of **1c** can be attributed to the strongest electron donating ability of *N*,*N*-diethylamino which produces largest molecular dipole. Moreover, the 2P fluorescence intensity of **1c** presents quadratic dependence on excitation power, which proved that the photoluminescence was from 2P process. (Fig. S1) Note that, since we didn't emphasize on comprehensive optimization of 2P fluorophores in this work, there should still have spaces to improve the 2PA property of HBI derivatives.

We further tested the photophysical property of **1c** in various solvents. The characteristic keto-form emission from ESIPT process is observed in aprotic solvents (e.g DMSO) while only the enol-form exists in protic solvents (e.g H_2O), which well matches the typical spectral characteristic of HBI moiety.[11] (Fig. S2a-b and Table S2) Therefore, **1c** has been proved for both 2PA and ESIPT properties, which makes it a potential platform for 2P fluorescent probe design. For the subsequent studies on the **1c**-based probe, we also measured the photoluminescence of **1c** in a series of DMSO-H_2O component solvent and found that 8:2 (DMSO/H_2O, V/V) was the optimized ratio to observe the keto-peak with large Stokes shift specific to ESIPT process. (Fig. S2c)

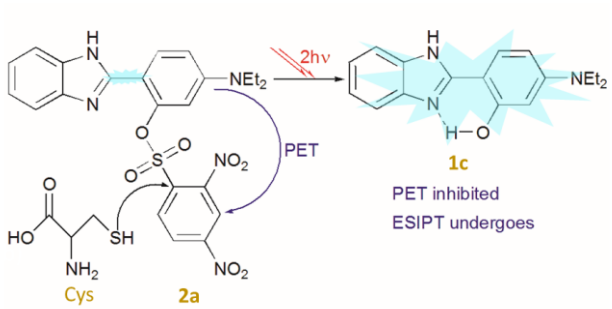

Scheme 2 The Cysteine (Cys) detection mechanism of probe **2a**.

As mentioned above, a significant change of ϕδ value would contribute to excellent performance in sensing and imaging applications of 2P fluorescent probes. For this purpose, we sought to obtain simultaneous enhancement of these two parameters. Hence we constructed an ESIPT-PET dual-mechanism 2P fluorescent probe: the probe-target reaction would deprive PET process and meanwhile activate ESIPT property. As a proof-of-concept illustration, we prepared a thiol probe **2a**, by linking 2,4-dinitrobenzenesulfoyl (DNBS, a well-known thiol recognition unit with high reactivity to thiolate anions[12]) to the 2'-hydroxyl of **1c**. We anticipated that the "on/off" switch of PET by removing DNBS and "off/on" control of ESIPT by releasing 2'-hydroxyl could be simultaneously achieved upon the cleavage of the sulfonate ester by thiol in nucleophilic aromatic substitution. (Scheme 2).

We firstly looked into the cysteine (Cys) assay under 1P mode. Only weak 1P fluorescence was observed with **2a** (ϕ=0.08) due to the occurrence of PET process. While for **1c**, the product of **2a**-Cys reaction, much higher quantum yield (ϕ=0.29) was detected because of the absence of PET (which will be discussed in detail later). When small increments of Cys were added into 10 μM **2a** in DMSO/HEPES (8/2, V/V, 10 mM, pH 7.4) component solvent, the 1P fluorescence was gradually enhanced and typical dual-peak of ESIPT molecules was observed (Fig. 1a). A maximal one-photon fluorescence enhancement factor (OFEF= $(F-F_{min})/F_{min}$) of ca. 19.0 was obtained in the presence of 50 μM Cys. We also measured the solubility of **2a** in water by fluorescence method[13], which was approximately 10 μM and enough for cell staining. (Fig. S3) Furthermore, both of probe **2a** and product **1c** were pH-insensitive at biological relevant pH range (Fig. S4a), which is also beneficial to bio-application. And we observed that the **2a**-Cys reaction reached the plateaus when pH value increased to 7.4, which can be explained by the enhanced nucleophilicity of sulphur atom in alkaline environment. (Fig. S4b) Consistent to reported thiol fluorescent probes using DNBS as recognition unit[8e,12e-f], probe **2a** showed positive responses to thiol compounds and negligible responses to thiol-free species with 100-fold excess. (Fig. S5)

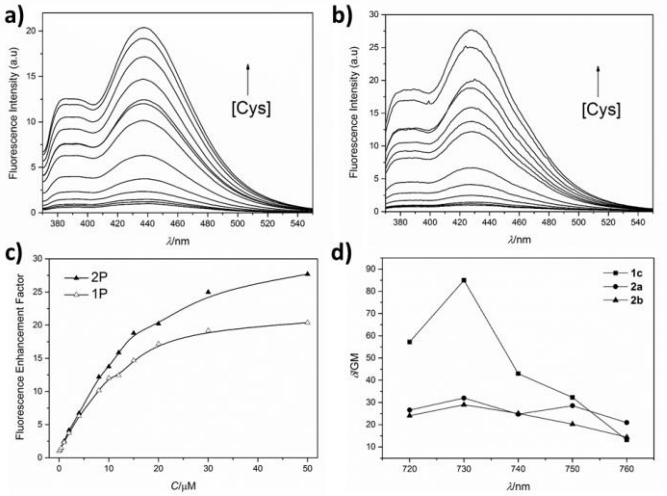

Fig. 1 a) 1P and b) 2P fluorescence changes of 10 μM **2a** in the presence of Cys with different concentrations. c) Comparison of fluorescence titration of 10 μM **2a** by increasing amount (0.2~50 μM) Cys. Above detection were performed in DMSO/HEPES (8/2, V/V, 10 mM, pH 7.4) and spectra were collected under 360 nm (1P mode) or 730 nm (2P mode) excitation light. d) 2P absorption cross section of **1c**, **2a** and **2b** under 720~760 nm excitation light (measured in DMSO).

We next investigated the fluorescence responses of **2a** toward Cys under 2P excitation. Fig. 1b shows the 2P fluorescence titration of 10 μM **2a** by Cys in DMSO/HEPES (8/2, V/V, 10 mM, pH 7.4), which is similar to the results in 1P titration. But an obvious difference between the 2P and 1P mode is the fluorescence enhancement factor. It is seen that the two-photon fluorescence enhancement factor (TFEF) value is larger than OFEF at each Cys concentration, and a maximal TFEF of ca. 26.0 was acquired with 50 μM Cys. (Fig. 1c) As known, the fluorescence response of 2P probes relies on the alteration of both ϕ and δ. Therefore, the more sensitive response of **2a** under 2P mode than 1P mode can be attributed mainly to the higher sensitivity of δ change under 2P excitation, since ϕ values under the two excitation modes are generally considered to be identical.

As we proposed above, the product (**1c**) of the probe **2a**-Cys reaction should possess higher molecular planarity than **2a**. To prove our assumption, we optimized the geometry of **1c** and **2a** using density functional theory (DFT) at the B3LYP/def2-SVP level by Orca.3.0.2[14], as drawn in Fig. 2a and Fig. 2b, respectively. It is intuitively observed that the three aromatic rings within **2a** are staggered to each other, while in **1c** the benzimidazole and phenol rings are in the same plane. Hence, we can explain the planarity enhancement during the probing process: the **2a** molecule is unable

to maintain the coplanar structure because the 2'-hydroxyl is linked to DNBS with considerable steric hindrance; whereas in the **1c** molecule, the free 2'-hydroxyl group generates an additional hydrogen-bond chelated ring so that the flat molecular geometry forms. As a result, π delocalization becomes more efficient in such locked conformation, thus promoting the target-induced 2.7-fold increase in δ_{max} value. (85 and 32 GM at 730 nm for **1c** and **2a**, respectively, as shown in Fig. 1d). It is worth pointing out that, although it is not hard to obtain a rigid planar structure and a large value of absorption cross section (up to hundreds or thousands GM) for 2P molecules, the absolute δ of 2P fluorophore is not decisive to the sensitivity of a 2P probe. Instead, the alteration of δ upon target reaction is the factor that really counts.

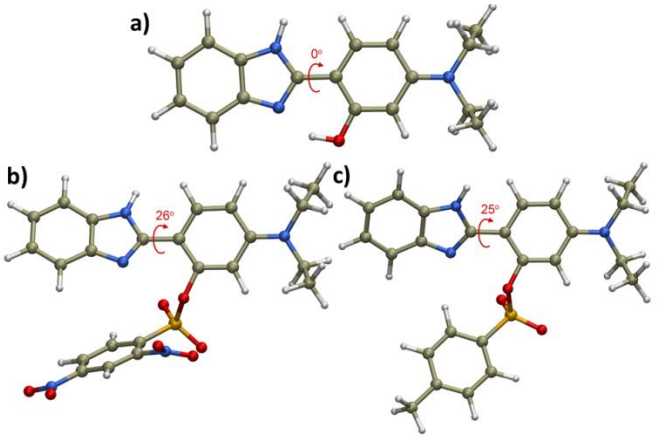

Fig. 2 Optimized geometries of a) **1c**, b) **2a**, and c) **2b** at the B3LYP/def2-SVP level by Orca.3.0.2. The dihedral angles between benzimidazole ring and phenyl ring of each molecule are displayed.

To further demonstrate the contribution to δ value by enhancement of molecular planarity as well as the contribution of PET to the rise of ϕ, we synthesized **2b** as a reference molecule. As seen from Fig. 2c, the absence of hydrogen bond and the steric hindrance provided by p-toluenesulfonyl group in **2b** produces a 25° dihedral angle between benzimidazole and phenyl rings, which is close to that of **2a** (26°). As a consequence, the δ value of **2b** (29 GM at 730 nm) is also similar to that of **2a**. On the other hand, the fluorescence quantum yield of **2b** (ϕ=0.17) is higher than **2a**, which we explain with the absence of PET process. To illustrate whether the PET process could occur in **1c**, **2a**, and **2b**, we calculated their energies of frontier orbitals at B3LYP/def2-SVP level by Orca.3.0.2. (Listed in Table S3). For **2a**, the HOMO is distributed on fluorophore (unreleased **1c**) and both of the LUMO and LUMO+1 are completely located on DNBS, which guarantees a typical PET process. When **2a** is excited, the electron transfers from excited fluorophore to DNBS, impeding the radiative relaxation and leading to fluorescence quenching. For **1c**, HOMO and LUMO are both located on the whole molecule, therefore the PET process does not occur. While for **2b**, the LUMO locates on p-toluenesulfonyl and HOMO and LUMO+1 mainly on fluorophore, hence the PET process is unlikely to undergo either. (The distribution of frontier orbitals and energy diagram of **1c**, **2a** and **2b** are drawn in Fig. S6 and S7)

With the simultaneous enhancement of ϕ and δ as well as the resultant TFEF in solution-phase Cys assay confirmed, we further thought to validate the rationality of our design by using probe **2a** for biothiols imaging in living cells. The cytotoxicity test by tetrazolium-based colorimetric assay (MTT) demonstrates negligible toxicity of probe **2a**. (Fig. S8) Next, the photostability of **2a** was detected in **2a**-labeled HeLa cells, which presented low photobleaching interference during the 40 min biothiol tracking. (Fig. S9) We then incubated 5 μM **2a** with HeLa cells to illuminate the endogenous biothiols. As controls, two groups of HeLa cells were separately pretreated with 0.5 mM exogenous Cys (positive group) and 1 mM *N*-methylmaleimide (NMM) acting as biothiols depleting agent (negative group), followed by incubation with 5 μM **2a**. Under 2P microscope, bright blue fluorescence was observed in cells stained with **2a**, and the positive and negative groups exhibited much brighter and weaker fluorescence, respectively (Fig. 3a-c, with the bright field and merged images shown in Fig. S10). The results confirmed the ability of probe **2a** to discriminate different concentrations of intracellular biothiols. The same groups were also observed under 1P microscope with identical incubation conditions (Fig. 3d-3f). Obviously, the contrast between the three groups under 2P mode is more distinct than that under 1P mode. The difference can also be read out from the normalized mean fluorescence intensity of 2P and 1P fluorescence images (separately shown in scale bars on the right lane of Fig. 3), as measured by Image-Pro Plus (v. 6.0). Especially, the contrast between the negative control and the sample group under 2P excitation (Fig. 3a and 3b) is much sharper than that under 1P excitation (Fig. 3d and 3e), indicating a significantly improved sensitivity contributed by the enhancement of δ. The result of imaging experiments is consistent with the above photophysical studies and solution assay results, which again validates that the ESIPT-PET dual-mechanism strategy could be an effective approach to improve TFEF and 2P probing performances. Another merit of this design, as mentioned above, is the relatively small size of the probe molecule. The fundamental studies on 2PA molecules suggest that a large δ always requires a large conjugate plane and/or a long conjugate chain of the molecule, which, however, leads to impaired water solubility and difficulty in cell experiments.[5] In this sense, the hydrogen bond in ESIPT molecules offering a flexible control of coplanar structure, which could be particularly suitable for the compromise of large δ and water solubility in 2P probes design.

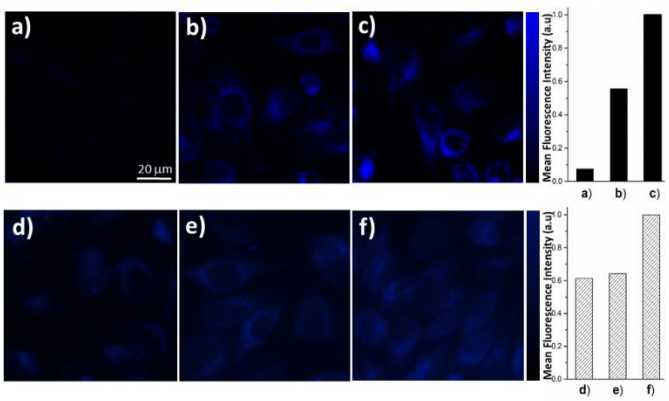

Fig. 3 Images of a), b) and c) are fluorescent images collected with 2P fluorescence microscopy. The excitation wavelength was 730 nm and images were collected at 400~500 nm. d)~f) Pseudocolor images from 1P fluorescence microscopy under UV light excitation mode. HeLa cells were incubated with a), d) 1 mM NMM and c), f) 0.5 mM Cys for 30 min before incubation with 5 μM probe **2a**. b), e) Cells were incubated with 5 μM **2a** without pretreatment. Bar graphs on right lane: normalized mean fluorescence density of images a)~f).

Conclusions

In conclusion, we developed a new strategy to design 2P fluorescent probes with simultaneously enhanced δ and ϕ after probe-target reaction. 2.7-fold enhancement of δ value was achieved by using a fluorophore with ESIPT property as the probe scaffold, which enabled target-induced increase of molecular planarity. Combined with the PET process, the dual-mechanism probe **2a** presented 26-fold fluorescence enhancement factor under two-photon excitation, which was higher than the 19-fold under one-photon excitation. Moreover, probe **2a** was applied in cell imaging for biothiols and showed better performance under two-photon microscope than one-photon microscope. Considering the feasibility to readily achieve reaction-based enhancement of molecular planarity by manipulating the intramolecular hydrogen bond, this work may open a new avenue to design 2P fluorescent probes for diverse targets. In this way, the absorption cross section can be elevated in addition to quantum yield, such that improved TFEF and more sensitive response of 2P probing can be expected.

The authors acknowledge the financial support from the National Natural Science Foundation of China (No. 21375098) and the National Basic Research of China (973 program, No. 2011CB933600)

Notes and references

[a] Key Laboratory of Analytical Chemistry for Biology and Medicine (Ministry of Education), College of Chemistry and Molecular Sciences, Wuhan University, Wuhan 430072, China.

[b] College of Life Science, Wuhan University, Wuhan 430072, China.

[c] Hubei Key Laboratory of Organic and Polymeric Optoelectronic Materials, College of Chemistry and Molecular Sciences, Wuhan University, Wuhan 430072, China.

† Electronic Supplementary Information (ESI) available: synthesis, photophysical experiments, molecular orbital calculation, bioimaging, cytotoxicity assay, and additional figures. See DOI: 10.1039/c000000x/

‡ These authors contributed equally to this work.

1. S. Yao and K. D. Belfield, *Eur. J. Org. Chem.*, **2012**, *2012*, 3199-3217.
2. H. M. Kim and B. R. Cho, *Acc. Chem. Res.*, **2008**, *42*, 863-872.
3. M. Albota, *Science*, **1998**, *281*, 1653-1656.
4. a) A. P. DeSilva, H. Q. N. Gunaratne, T. Gunnlaugsson, A. J. M. Huxley, C. P. McCoy, J. T. Rademacher and T. E. Rice, *Chem. Rev.*, **1997**, *97*, 1515-1566. b) H. M. Kim and B. R. Cho, *Chem. Asia. J.*, **2011**, *6*, 58-69.
5. a) H. M. Kim and B. R. Cho, *Chem. Commun.*, **2009**, 153-164. b) M. Pawlicki, H. A. Collins, R. G. Denning and H. L. Anderson, *Angew. Chem. Int. Ed.*, **2009**, *48*, 3244-3266.
6. a) R. Zalesny, W. Bartkowlak, S. Styrcz and J. Leszczynski, *J. Phys. Chem. A.*, **2002**, *106*, 4032-4037. b) S. K. Pati, T. J. Marks and M. A. Ratner, *J. Am. Chem. Soc.*, **2001**, *123*, 7287-7291.
7. a) O. Mongin, L. Porres, M. Charlot, C. Katan and M. Blanchard-Desce, *Chem. Eur. J.*, **2007**, *13*, 1481-1498. b) K. S. Kim, J. M. Lim, A. Osuka and D. Kim, *J. Photochem. Photobiol., C.*, **2008**, *9*, 13-28. c) I. Hisaki, S. Hiroto, K. S. Kim, S. B. Noh, D. Kim, H. Shinokubo and A. Osuka, *Angew. Chem. Int. Ed.*, **2007**, *46*, 5125-5128. d) Z. Fang, T. L. Teo, L. P. Cai, Y. H. Lai, A. Samoc and M. Samoc, *Org. Lett.*, **2009**, *11*, 1-4. e) T. K. Ahn, K. S. Kim, D. Y. Kim, S. B. Noh, N. Aratani, C. Ikeda, A. Osuka and D. Kim, *J. Am. Chem. Soc.*, **2006**, *128*, 1700-1704.
8. a) J. E. Kwon and S. Y. Park, *Adv. Mat.*, **2011**, *23*, 3615-3642. b) J. Z. Zhao, S. M. Ji, Y. H. Chen, H. M. Guo and P. Yang, *Phys. Chem. Chem. Phys.*, **2012**, *14*, 8803-8817. c) R. Hu, J. Feng, D. H. Hu, S. Q. Wang, S. Y. Li, Y. Li and G. Q. Yang, *Angew. Chem. Int. Ed.*, **2010**, *49*, 4915-4918. d) Y. P. Chan, L. Fan, Q. H. You, W. H. Chan, A. W. M. Lee and S. M. Shuang, *Tetrahedron*, **2013**, *69*, 5874-5879; e) M. H. Lan, J. S. Wu, W. M. Liu, H. Y. Zhang, W. J. Zhang, X. Q. Zhuang and P. F. Wang, *Sens. Actuators, B.*, **2011**, *156*, 332-337
9. C. C. Hsieh, C. M. Jiang and P. T. Chou, *Acc. Chem. Res.*, **2010**, *43*, 1364-1374.
10. a) F. Gao, X. C. Wang, H. R. Li and X. J. Ye, *Tetrahedron*, **2013**, *69*, 5355-5366. b) M. Tasior, V. Hugues, M. Blanchard-Desce and D. T. Gryko, *Chem. Asia. J.*, **2012**, *7*, 2656-2661. c) J. J. Zheng, Y. X. Guo, X. P. Li, G. L. Zhang and W. J. Chen, *J. Opt. A: Pure Appl. Opt.*, **2006**, *8*, 835-839. d) F. Wu, L. Ma, S. W. Zhang, Y. H. Geng, J. Lü and X. M. Cheng, *Chem. Phys. Lett.*, **2012**, *519-520*, 141-144. e) Y. Q. Tian, C. Y. Chen, C. C. Yang, A. C. Young, S. H. Jang, W. C. Chen and A. K. Jen, *Chem. Mater.*, **2008**, *20*, 1977-1987.
11. M. Fores, M. Duran, M. Sola, M. Orozco and F. J. Luque, *J. Phys. Chem. A.*, **1999**, *103*, 4525-4532.
12. a) C. C. Zhao, Y. Zhou, Q. N. Lin, L. Y. Zhu, P. Feng, Y. L. Zhang and J. Cao, *J. Phys. Chem. B.*, **2011**, *115*, 642-647. b) H. Maeda, H. Matsuno, M. Ushida, K. Katayama, K. Saeki and N. Itoh, *Angew. Chem. Int. Ed.*, **2005**, *44*, 2922-2925. c) H. Maeda, K. Katayama, H, Matsuno and T. Uno, *Angew. Chem. Int. Ed.*, **2006**, *45*, 1810-1813. d) W. Jiang, Q. Q. Fu, H. Y. Fan, J. Ho and W. Wang, *Angew. Chem.*, **2007**, *119*, 8597-8600. e) Y. H. Chen, J. Z. Zhao, H. M. Guo and L. J. Xie, *J. Org. Chem.*, **2012**, *77*, 2192-2206. f) H. M. Guo, Y. Y. Jing, X. L. Yuan, S. M. Ji, J. Z. Zhao, X. H. Li and Y. Y. Kan, *Org. Biomol. Chem.*, **2011**, *9*, 3844-3853.
13. H. M. Kim, H. J. Choo, S. Y. Jung, Y. G. Ko, W. H. Park, S. J. Jeon, C. H. Kim, T. Joo and B. R. Cho, *Chembiochem.*, **2007**, *8*, 553-559.
14. F. Neese, *WIREs. Comput. Mol. Sci.*, **2012**, *2*, 73-78.

